

Phase, microstructure and ferroelectric properties of new complex-structured ferroelectric ceramics in the PZT–SBN system

Orapim Namsar^a, Anucha Watcharapasorn^{a,b}, Sukanda Jiansirisomboon^{a,b,*}

^aDepartment of Physics and Materials Science, Faculty of Science, Chiang Mai University, Chiang Mai 50200, Thailand

^bMaterials Science Research Center, Faculty of Science, Chiang Mai University, Chiang Mai 50200, Thailand

Available online 17 October 2012

Abstract

This study aimed to fabricate and characterize new complex-structured ceramics with formula $(1-x)\text{Pb}(\text{Zr}_{0.52}\text{Ti}_{0.48})\text{O}_3-x\text{SrBi}_2\text{Nb}_2\text{O}_9$ or $(1-x)\text{PZT}-x\text{SBN}$ (where $x=0, 0.1, 0.3$ and 0.5 weight fraction). The ceramics were prepared by a solid-state mixed-oxide method and sintered at temperatures between 1000 and 1250°C . Optimum sintering temperature for this system was found to be 1050°C for 3 h dwell time. X-ray diffraction patterns of $(1-x)\text{PZT}-x\text{SBN}$ powders showed peak intensities of two-phase mixture corresponding to the relative amount of each phase as a result of SBN addition. Microstructure of $(1-x)\text{PZT}-x\text{SBN}$ ceramics showed a variation in grain shape and grain size. The small addition of SBN ($x=0.1$) was also found to improve ferroelectric properties of pure PZT ceramic.
© 2012 Elsevier Ltd and Techna Group S.r.l. All rights reserved.

Keywords: A. Sintering; B. X-ray methods; C. Ferroelectric properties

1. Introduction

Nowadays, ferroelectric materials are widely applied in electronic device applications, e.g. sensors, actuators and non-volatile random access memories [1]. Many of these applications require materials with superior ferroelectric properties. It has been well-known that isotropic perovskite structure and bismuth layered structure compounds are two important ferroelectric materials used in these applications.

A perovskite structure compound, i.e. lead zirconate titanate (PZT), exhibits excellent ferroelectric properties such as high remanent polarization but it has low fatigue resistance [2,3]. The structure of bismuth layered structured ferroelectrics (BLSFs) revealed that strontium bismuth niobate (SBN) and strontium bismuth tantalate (SBT) consist of $(\text{Bi}_2\text{O}_2)^{2+}$ layer interleaved with perovskite-like block $(\text{SrNb}_2\text{O}_7)^{2-}$ and $(\text{SrTa}_2\text{O}_7)^{2-}$, respectively [4]. Both ferroelectric SBT and SBN exhibit excellent fatigue resistance and low leakage current [5]. However, compared to

the traditional PZT solid solution system, their ferroelectric properties were not favourable due to inherently small saturated and remanent polarizations, and requirement of a relatively high processing temperature.

Many research groups have attempted to combine the perovskite structure and bismuth layered structure compound together in a form of ceramic such as PZT–SBT [6], PLZT–SBT [7] and PLZT–SBN [8]. These results indicated that the binary ceramic systems had better ferroelectric and dielectric properties over those of pure PZT and PLZT ceramics. In the present study, a series of new ceramics with formula $(1-x)\text{PZT}-x\text{SBN}$ (where $x=0, 0.1, 0.3$ and 0.5 weight fraction) were fabricated and characterized particularly in terms of phase evolution, density, microstructural changes and ferroelectric properties.

2. Material and methods

The $\text{Pb}(\text{Zr}_{0.52}\text{Ti}_{0.48})\text{O}_3$ (PZT) and $\text{SrBi}_2\text{Nb}_2\text{O}_9$ (SBN) powders were prepared by a solid-state mixed-oxide method. The starting chemicals used were PbO (99%, Fluka), ZrO_2 (99%, Riedel-de Haëln), TiO_2 (99%, Riedel-de Haëln), SrCO_3 (98%, Aldrich), Bi_2O_3 (98%, Fluka) and Nb_2O_5 (99%, Aldrich). The starting powders were weighed,

*Corresponding author at: Department of Physics and Materials Science, Chiang Mai University, Faculty of Science, Chiang Mai 50200, Thailand.

E-mail address: sukanda.jian@cmu.ac.th (S. Jiansirisomboon).

ball-milled in ethanol for 24 h and oven dried. The mixed powders were calcined at 800 °C for 2 h for PZT and 950 °C for 3 h for SBN powders. The calcined PZT and SBN powders were then weighed, mixed by ball-milling and dried to produce the powder mixture of $(1-x)\text{PZT}-x\text{SBN}$, where $x=0, 0.1, 0.3$ and 0.5 weight fraction. Each mixture was pressed into pellets with 3 wt% (polyvinyl alcohol or PVA) added as a binder. These pellets were covered with their own powders and sintered at 1050 °C for 3 h. Phase characterization of $(1-x)\text{PZT}-x\text{SBN}$ ceramics was carried out using X-ray diffractometry (XRD, Phillip Model X-pert). Density of ceramics was determined using Archimedes' method. The microstructure and chemical composition of sintered samples were examined using scanning electron microscopy (SEM, JEOL JSM-6335F) and energy dispersive X-ray spectroscopy (EDS) techniques. Average grain size was determined using a caliper diameter method from SEM micrographs. Ferroelectric hysteresis (P – E) loops were characterized at a frequency of 50 Hz using a computer-controlled modified Sawyer–Tower circuit. Remanent polarization (P_r), maximum polarization (P_{max}), coercive field (E_c), maximum field (E_{max}) and loop squareness (R_{sq}) values were then determined from the hysteresis loops. The squareness ratio of the hysteresis loop were calculated using the ratio of P_r at zero electric field to saturated polarization (P_s) obtained at some finite field strength below dielectric breakdown, i.e. P_r/P_s . For a not fully saturated loop, P_s was assumed to be equal to P_{max} . According to Haertling and Zimmer [9], the squareness could be used to measure not only the deviation in the polarization axis but also that in the electric field axis with an empirical equation: $R_{\text{sq}} = (P_r/P_s) + (P_{1.1E_c}/P_r)$.

3. Results and discussion

Fig. 1 shows the X-ray diffraction patterns of $(1-x)\text{PZT}-x\text{SBN}$ powders at different x compositions. Phase of PZT powder showed a co-existence of rhombohedral (ICSD file no. 97060) and tetragonal (ICSD file no. 92059) phases. For other compositions, all X-ray patterns showed peaks of two-phase mixture of PZT and orthorhombic SBN phase (ICSD file no. 88473). It is seen that the intensity of SBN peaks increase with increasing its concentration. X-ray diffraction patterns of the ceramics sintered at 1050 °C for 3 h are shown in Fig. 2. The X-ray diffraction patterns of perovskite PZT ceramics was identified as a single-phase material with only tetragonal symmetry. The disappearance of a rhombohedral symmetry in this ceramic is believed to be caused by changes in compositional stoichiometry due to high sintering temperature [10]. For the samples with $x=0.1\text{SBN}$, the crystalline were indexed to be the PZT-based solid solution as a main phase with a minor phase of new multinary compound. The new multinary compound matches the standard JCPDS diffraction data of $\text{Pb}_2(\text{Nb}_{1.33}\text{Ti}_{0.66})\text{O}_{6.66}$ (no. 74-0660) which has a cubic symmetry. This phase appears as a result of reaction between PZT and SBN phases. The PZT peaks was shifted to higher angles, implying that a small amount

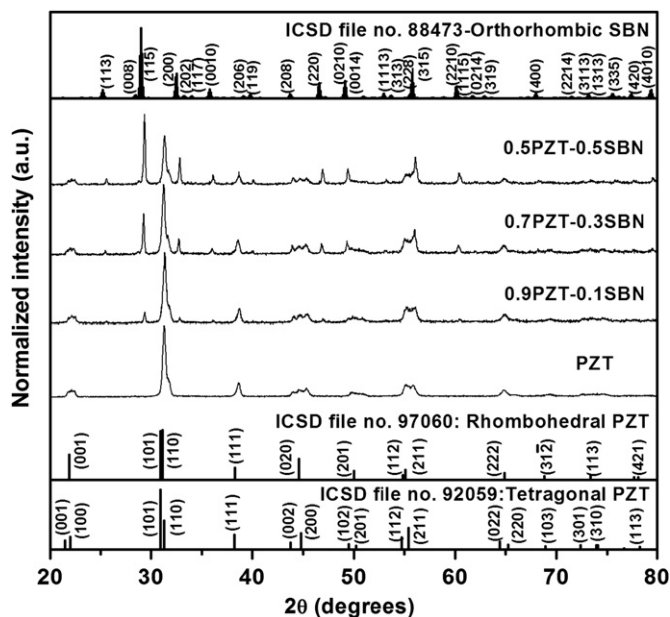


Fig. 1. X-ray pattern of $(1-x)\text{PZT}-x\text{SBN}$ powders.

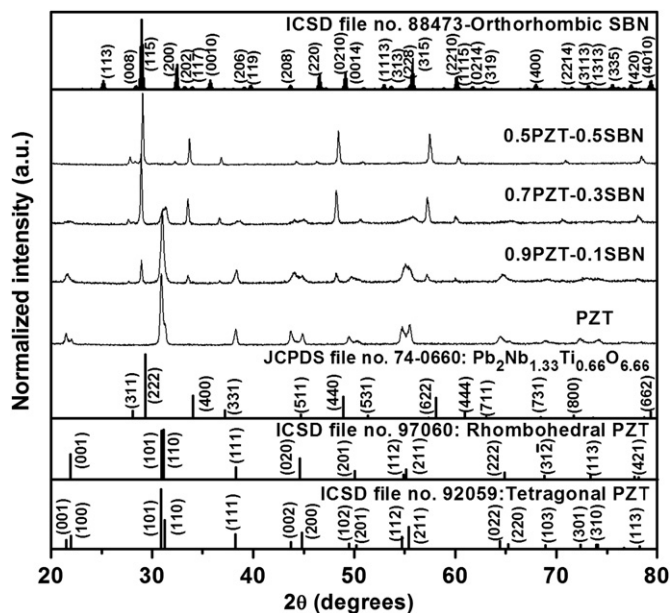


Fig. 2. X-ray pattern of $(1-x)\text{PZT}-x\text{SBN}$ ceramics.

of SBN was dissolved into PZT to form PZT-rich solid solution. Addition of $x=0.3\text{SBN}$ into this compound caused a shift of PZT peaks to higher angles with a reduction in intensities, while a new multinary phase was maintained with a rapid increase in intensities. This result suggested that a small amount of SBN may dissolve into PZT to form PZT-rich solid solution. In the same manner, a certain amount of PZT may also dissolve into SBN to form a new solid solution phase. An increase in SBN concentration to $x=0.5$ showed a composite structure between a new multinary compound and SBN compound. However, the PZT-based solid solution started to disappear

in this sample. This result implied that PZT was completely dissolved into SBN structure to form a new multinary solid solution phase.

Bulk density of the $(1-x)\text{PZT}-x\text{SBN}$ ceramics are listed in Table 1. It was observed that the sample with $x=0.1\text{SBN}$ showed a higher density than other compositions. Further increase in content of SBN leads to a gradual decrease in the densities of the ceramics. The result indicated that SBN content has a significant effect on densification of PZT–SBN ceramics.

SEM micrographs of thermally etched surfaces of $(1-x)\text{PZT}-x\text{SBN}$ ceramics are shown in Fig. 3. PZT ceramic possessed normal equiaxed shape with an average grain size of $\sim 4.09\text{ }\mu\text{m}$. The sample with $x=0.1\text{SBN}$ contained a two phase mixture of different grain shape and size. An equiaxed shape grains and polyhedral-shape grains were assigned (EDS analysis—not shown here) to the PZT phase and new multinary phase. This sample exhibited a good densification, a homogenous grain size and a uniform grain packing. Clearly, this was a reason for a higher density obtained in this composition. For the sample with $x=0.3\text{SBN}$, the equiaxed shape grain of PZT

and polyhedral shape grain of new multinary phase were observed. For the grain size observation of this sample, it showed a rapid increase of grain size of the new multinary phase, while the grain size of PZT phase decreased (see Table 1). However, a high porosity and an heterogeneous microstructure consisting of two phases were found in this sample. The sample with $x=0.5\text{SBN}$ consisted mainly of polyhedral-shaped grains of new multinary compound and a small amount of plate-like grains of SBN. This sample exhibits a low packing density due to a large difference in grain shape of polyhedral and plate-like grains. The SEM analysis results are consistent with the density values and the X-ray studies.

Hysteresis loops of $(1-x)\text{PZT}-x\text{SBN}$ ceramics are shown in Fig. 4. The related ferroelectric parameters are also listed in Table 2. The shape of P – E loops varies greatly with the ceramic compositions. PZT ceramics showed a ferroelectric loop with 8.29 kV/cm of coercive field (E_C), $10.14\text{ }\mu\text{C/cm}^2$ of remanent polarization (P_r) and 0.74 of loop squareness (R_{sq}). The composition with $x=0.1\text{SBN}$ exhibits an enhanced ferroelectric behaviour i.e. $E_C=14.05\text{ kV/cm}$, $P_r=13.19\text{ }\mu\text{C/cm}^2$ and $R_{sq}=1.14$. The improvement

Table 1
Density and grain size of $(1-x)\text{PZT}-x\text{SBN}$ ceramics.

Composition	Bulk density (gcm^{-3})	Grain size (μm)				
		Equiaxed shape	Polyhedral shape		Plate-liked shape	
		Diameter (ϕ)	Width (d)	Length (l)	Width (d)	Length (l)
PZT	7.55 ± 0.01	4.09 ± 0.23	–	–	–	–
$0.9\text{PZT}-0.1\text{SBN}$	7.63 ± 0.05	1.34 ± 0.05	1.41 ± 0.15	1.34 ± 0.14	–	–
$0.7\text{PZT}-0.3\text{SBN}$	7.18 ± 0.04	1.04 ± 0.06	2.53 ± 0.18	2.98 ± 0.22	–	–
$0.5\text{PZT}-0.5\text{SBN}$	6.94 ± 0.01	–	2.45 ± 0.17	2.92 ± 0.14	0.33 ± 0.03	1.29 ± 0.09

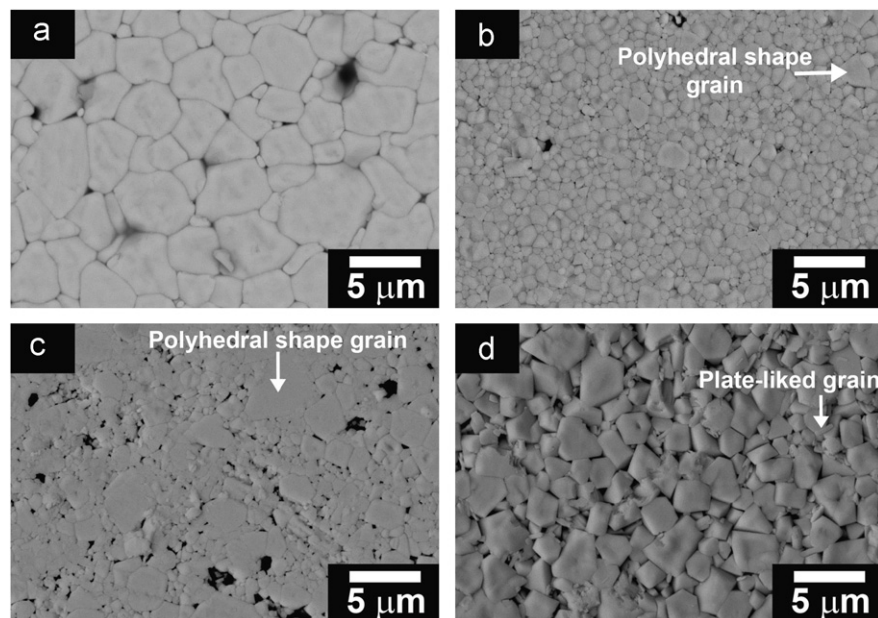


Fig. 3. Microstructure of $(1-x)\text{PZT}-x\text{SBN}$ ceramics, where (a)–(d) represent $x=0, 0.1, 0.3$ and 0.5 weight fraction, respectively.

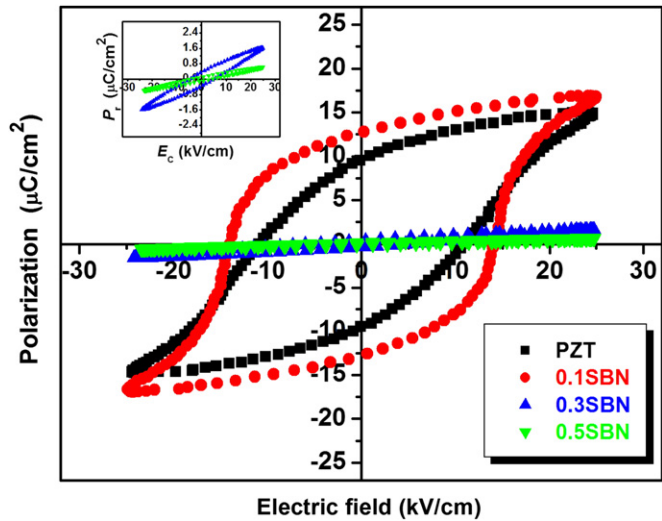


Fig. 4. Hysteresis loop of (1-x)PZT-xSBN ceramics.

Table 2
Ferroelectric properties of (1-x)PZT-xSBN ceramics.

Composition	P_r ($\mu\text{C}/\text{cm}^2$)	E_C (kV/cm)	R_{sq}
PZT	10.14	8.29	0.74
0.9PZT–0.1SBN	13.19	14.50	1.14
0.7PZT–0.3SBN	0.39	5.51	0.25
0.5PZT–0.5SBN	0.12	4.24	0.20

in ferroelectric properties in this composition was mainly attributed to donor-like ionic substitution [1]. Moreover, the small grain size and a slight change in crystal structure also partially contributed to the improved ferroelectric behavior. Upon further increasing the SBN content from $x=0.3$ to 0.5, the ferroelectric properties of the PZT–SBN system degrades. This result was mainly due to an increase amount of a cubic phase, as observed in XRD and microstructural studies. It is well-known that the material with cubic symmetry can not possess ferroelectric properties. A degradation of the ferroelectric properties of these samples was confirmed by a slimmer hysteresis loops. Apparent phase transition and microstructural changes were the main factors that determines the ferroelectric properties of this new material system.

4. Conclusions

In this study, (1-x)PZT-xSBN ceramics were successfully prepared by a solid-state mixed-oxide method. PZT ceramic showed only tetragonal symmetry. The composition

with $0.1 \leq x \leq 0.3$ showed a composite structure of PZT-based solid solution and new multinary phase. Addition of 0.5SBN into PZT showed a two phase mixture of new multinary phase and small amount of SBN phase. The microstructural changes were in agreement with the observed X-ray diffraction patterns. The maximum ferroelectric properties were achieved at the sample with PZT-based solid solution region (i.e. 0.1SBN). The improvement in ferroelectric properties was mainly due to donor-like ionic substitution.

Acknowledgments

This work is financially supported by The Thailand Research Fund (TRF) and the National Research University Project under Thailand’s Office of The Higher Education Commission (OHEC). The Faculty of Science and the Graduate School, Chiang Mai University is also acknowledged. O. Namsar would like to acknowledge financial support from the TRF through the Royal Golden Jubilee Ph.D. Program.

References

[1] G.H. Haertling, Ferroelectric ceramics: history and technology, *Journal of the American Ceramic Society* 82 (4) (1999) 797–818.
[2] O. Auciello, J.F. Scott, R. Ramesh, The physics of ferroelectric memories, *Physics Today* 51 (1998) 22–27.
[3] D.H. Bao, N. Wakiya, K. Shinozaki, N. Mizutani, X. Yao, Abnormal ferroelectric properties of compositionally graded $\text{Pb}(\text{Zr,Ti})\text{O}_3$ thin films with LaNiO_3 bottom electrodes, *Journal of Applied Physics* 90 (2001) 506–508.
[4] L. Sun, C. Feng, L. Chen, S. Huang, X. We, Piezoelectric and ferroelectric properties of $\text{SrBi}_2(\text{Nb}_{1-x}\text{Ta}_x)_2\text{O}_9$ ceramics, *Materials Science and Engineering B* 135 (2006) 60–64.
[5] C.A.P. de Araujo, L.D. McMillan, J.D. Cuchiaro, M.C. Scott, J.F. Scott, Fatigue free ferroelectric capacitors with platinum electrodes, *Nature* 374 (1995) 627–629.
[6] X.M. Chen, J.S. Yang, Composite piezoelectric ceramics in the PZT– $\text{SrBi}_2\text{Ta}_2\text{O}_9$ system, *Journal of Materials Science* 8 (1997) 147–150.
[7] N. Zhang, L.T. Li, B. Li, D. Guo, Z. Gui, Improvement of electrical fatigue properties in PLZT ferroelectric ceramics due to $\text{SrBi}_2\text{Ta}_2\text{O}_9$ incorporation, *Materials Science and Engineering B* 90 (2002) 185–190.
[8] N. Zhang, L. Li, Z. Gui, Improvement of electric fatigue in $\text{Pb}_{0.94}\text{La}_{0.04}(\text{Zr}_{0.70}\text{Ti}_{0.30})\text{O}_3$ ferroelectric capacitors due to $\text{SrBi}_2\text{Nb}_2\text{O}_9$ incorporation, *Materials Research Bulletin* 36 (2001) 2553–2526.
[9] G.H. Haertling, W.J. Zimmer, An analysis of hot-pressing parameters for lead zirconate-lead titanate ceramics containing two atom percent bismuth, *American Ceramic Society Bulletin* 45 (1966) 1084–1089.
[10] J.C. Fernandes, D.A. Hall, M.R. Cockburn, G.N. Greaves, Phase coexistence in PZT ceramic powders, *Nuclear Instruments and Methods B* 97 (1995) 137–141.